Dynamical templates for comparison to Λ CDM: Static or dynamical dark energy?

Rodger I. Thompson

Steward Observatory and Department of Astronomy, University of Arizona 933 N. Cherry Ave., Tucson Arizona, USA

E-mail: rit@email.arizona.edu

Abstract. This study forges new tools to discriminate between dynamical and static dark energy. It provides accurate evolutionary templates of dynamical cosmological parameters and fundamental constants as analytic functions of the scale factor. They are designed to replace the commonly used parameterizations in likelihood calculations with evolutionary templates based on the physics of specific dynamical cosmologies and dark energy potentials. Thus they are termed Cosmology and Potential Specific, CPS, templates. A suite of CPS templates are calculated for a flat quintessence cosmology with a dark energy potential of the same mathematical form as the Higgs potential. This Higgs inspired, HI, polynomial potential produces a rich set of evolutions unlike most monomial potentials. The study produces CPS templates that are analytic functions of the scale factor. It uses a recently developed beta function formalism that provides a differential function for the scalar in terms of the scale factor. This establishes a methodology for easily producing CPS templates for other dark energy potentials and cosmologies to determine the likelihoods of dynamical cosmologies relative to Λ CDM. The study also examines the evolution of fundamental constants such as the proton to electron mass ratio and the fine structure constant involving an intersection between particle physics and cosmology. Appendix A displays an abridged suite of CPS templates for flat quintessence and the HI dark energy potential.

Keywords: Dark energy theory, particle physics - cosmology connection

\mathbf{C}_{0}	contents						
1	Introduction	2					
2	The specific cosmology and potential	3					
	2.1 Flat quintessence	3					
	2.1.1 The Friedmann constraints	3					
	2.2 The HI potential	4					
3	The Need for CPS Templates	4					
4	The beta function formalism						
	4.1 The beta function	5					
	4.1.1 The HI potential beta function	6					
5	Parameter evolution derivations	7					
	5.1 $\kappa\theta$ as a function of the scale factor	7					
	5.1.1 The beta function in terms of the Lambert W function	8					
	5.1.2 Calculation of the potential constant M	9					
	5.2 The beta dark energy potential	9					
	5.3 The Hubble Parameter	10					
	5.4 The derivatives of θ	10					
	5.5 The dark energy density and pressure and the matter density	11					
	5.6 The Dark Energy Equation of State	11					
	5.7 The CPS templates	12					
6	Cosmological Parameter Evolution and Observations						
	6.1 Boundary conditions and constants	12					
	6.2 The evolution of the scalar	13					
	6.3 The evolution of the dark energy potential	13					
	6.4 The accuracy of the CPS templates	14					
	6.5 The evolution of the Hubble parameter	15					
	6.5.1 Deviations from ΛCDM	15					
	6.5.2 Hubble parameter observational implications	16					
	6.6 Evolution of $\dot{\theta}$	16					
	6.7 Evolution of the dark energy density	17					
	6.8 Evolution of the dark energy equation of state	18					
7	•	19					
	7.1 Fundamental constant cosmological and new physics constraints	20					
8	Conclusions	21					
\mathbf{A}	CPS templates in $W(\chi)$	24					

1 Introduction

The decadal review of astrophysics and astronomy for the 2020s [1] identifies the question of whether the dark energy density of the universe is static or dynamic as one of the great unanswered questions in modern science. The answer requires an accurate comparison of the relative likelihoods of Λ CDM and dynamical cosmologies. The predicted evolutions of cosmological parameters, templates, for Λ CDM are well known based on general relativity and the standard model of physics. Calculations of the likelihood of dynamical cosmologies, however, are most often based on parameterizations rather than the physics of the cosmologies and dark energy potentials. Proper scientific inquiry requires likelihoods based on the physics of the cosmology and dark energy potential that is being tested. This study presents a methodology for achieving that goal. It demonstrates the methodology by calculating evolutionary templates for a specific dynamical cosmology and dark energy potential that provide significant improvements over the current parameterizations. The need for Cosmology and Potential Specific, CPS, templates is discussed in section 3 in terms of the current parameterization for the dark energy equation of state, EoS. Evolutions of cosmological parameters such as the dark energy EoS, w, are strong functions of both the cosmology and the dark energy potential. The multiplicity of dynamical cosmologies and number of possible dark energy potentials has been one of the sticking points hindering the development of dynamical templates. The methodology in this work simplifies calculating accurate evolutionary CPS templates. The well studied flat quintessence dynamical cosmology provides a logical starting point for the study. The dark energy potential has the same mathematical form as the Higgs potential, $V(\phi) \propto (\phi^2 - \gamma^2)^2$, and is therefore referred to as the Higgs Inspired or HI potential in subsequent discussion. The value of the constant γ is greater than the current scalar ϕ_0 placing the equilibrium point $\phi = \gamma$ in the future. At early times the constant γ^4 term dominates, acting as a cosmological constant until the dynamical terms produce significant evolution during the late times, $z \leq 10$, considered here. The detailed properties of the HI potential are examined in section 2.2.

For likelihood calculations the CPS templates should be accurate, analytic and functions of an observable cosmological variable such as the scale factor a or redshift z. The scale factor a=0.1-1.0 is the variable used in this study. The recently developed beta function formalism [2–4], presented in section 4, is the key to templates that are functions of the scale factor a. It provides a methodology for creating the templates in a simple manner that overcomes the problem of the multitude of dynamical cosmologies and dark energy potentials. Extension of the methodology to DBI and non-standard kinetic term cosmologies has been accomplished by [5]. Cosmologies with non-minimal couplings have been also addressed [3]. The formalism has its origins in particle physics renormalization studies [3]. The cosmological beta function is a function of the scalar ϕ and the scale factor a that provides a differential equation to solve for $\phi(a)$. The details of the beta function formalism in a quintessence cosmology are presented in section 4.

The primary purpose of CPS templates is likelihood calculations. They, however, play important roles in other areas such as observation planning where accurate templates indicate the best redshift regions for measurements and the accuracy needed to discriminate between static and dynamical dark energy. They also indicate which cosmological parameters are sensitive measures of dark energy and which are not. The range of evolution is also indicated by the CPS templates such as the perhaps unexpected non-monotonic evolution of the dark energy EoS for some of the cases in this study. CPS templates also serve as the initial solution

for numerical exact solutions to the cosmology and potential. This may occur for cosmologies and potentials that have a high likelihood.

Natural units are used throughout with c, \hbar and $8\pi G$ set to one. Masses are given in terms of reduced Planck masses, M_p and the constant κ is defined as $\frac{1}{M_p}$. In the adopted mass units κ is equal to one but is retained in equations and relevant text to properly indicate the units.

2 The specific cosmology and potential

The specific cosmology and potential in this study is flat quintessence with a dark energy potential that has the mathematical form of the Higgs potential. Quintessence is well developed [6, 7] and a basic example of a dynamical scalar field dark energy cosmology. The HI potential's mathematical relation to the Higgs has a degree of naturalness that makes it physically motivated. The analysis and CPS templates developed are based on the physics of this specific cosmology and potential rather than a parameterization.

2.1 Flat quintessence

A few quintessence features used in this study are given here for convenience. The quintessence dark energy density, ρ_{ϕ} , and pressure, P_{ϕ} equations are in terms of the scalar ϕ with units of mass and the potential with units of mass⁴.

$$\rho_{\phi} \equiv \frac{\dot{\phi}^2}{2} + V(\phi), \qquad P_{\phi} \equiv \frac{\dot{\phi}^2}{2} - V(\phi) \tag{2.1}$$

where $\dot{\phi}$ has units of mass squared. The dark energy EoS $w(\phi)$ is

$$w(\phi) = \frac{P_{\phi}}{\rho_{\phi}} = \frac{\frac{\dot{\phi}^2}{2} - V(\phi)}{\frac{\dot{\phi}^2}{2} + V(\phi)}.$$
 (2.2)

Combining eqns. 2.1 gives

$$P_{\phi} + \rho_{\phi} = \dot{\phi}^2 \tag{2.3}$$

It follows that

$$\frac{P_{\phi} + \rho_{\phi}}{\rho_{\phi}} = w + 1 = \frac{\dot{\phi}^2}{\rho_{\phi}} \tag{2.4}$$

giving $\dot{\phi}$ a relationship to the dark energy EoS and the dark energy density.

$$\dot{\phi}^2 = \rho_\phi(w+1) \tag{2.5}$$

2.1.1 The Friedmann constraints

In addition to the quintessence specific relations the two Friedmann constraints play an important role in the methodology. The forms of the first and second Friedman constraints used here are

$$3H^{2}(a) = \rho_{\phi}(a) + \rho_{m}(a) \qquad 3(\dot{H}(a) + H(a)^{2}) = -\frac{\rho(a) + 3P(a)}{2}$$
 (2.6)

where $\rho_{\phi}(a)$ is the dark energy density, $\rho_{m}(a)$ is the matter density, $\rho(a)$ is the sum of the matter and dark energy densities and P(a) is the dark energy pressure.

2.2 The HI potential

The model HI potential is given in a modified Ratra Peebles format [8, 9].

$$V(\theta) = M^{4}((\kappa\theta)^{2} - (\kappa\delta)^{2})^{2} = M^{4}((\kappa\theta)^{4} - 2(\kappa\theta)^{2}(\kappa\delta)^{2} + (\kappa\delta)^{4})$$
 (2.7)

The constant M has units of mass and contains all of the dimensionality of the potential. The true scalar ϕ is related to θ by $\phi = M\kappa\theta$ and the true constant γ is related to δ by $\gamma = M\kappa\delta$. The designations θ and δ are used to indicate that they are not the true scalar and constant. M is not a free parameter but is determined by the boundary conditions and the first Friedmann constraint. The scalar θ and the constant δ also have units of mass, hence $\kappa\theta$ and $\kappa\delta$ are dimensionless, eliminating the need for the n in the usual M^{4+n} notation of the Ratra-Peebles format. In this format $\kappa\theta$ and $\kappa\delta$ have magnitudes on the order of unity while M is on the order of $10^{-31}M_p$. The format was partially chosen to make the derived CPS templates compatible with multiple standard mathematical platforms although the Mathematica platform used in this study easily handles the order of 10^{-121} values encountered in the calculations. The true scalar ϕ in the potential is the dark energy scalar field with none of the complex physics associated with the Higgs field. The remainder of the study utilizes θ and δ to be consistent with the CPS templates.

Since $\delta > \theta$ the constant $(\kappa \delta)^4$ term is dominant. The scalar θ is much smaller than δ at early times therefore the $(\kappa \delta)^4$ term acts like a cosmological constant in early evolution. The dynamical $-2(\kappa \theta)^2(\kappa \delta)^2$ term is the next largest term and provides the rolling of the potential to smaller values at later times. For the scale factor range considered here the dynamical $(\kappa \theta)^4$ is always subdominant but can influence the second derivative of the evolution.

3 The Need for CPS Templates

An important example of the need for CPS templates is the ubiquitous Chevallier, Polarski, Linder, CPL, [10, 11] linear parameterization of w given by

$$w(a) = w_o + (1 - a)w_a (3.1)$$

CPL is the preferred parameterization of w for a majority of new missions and facilities e.g. [12].

Its linear form is quite adequate for testing the validity of ΛCDM and any deviation of w_0 from minus one or w_a from zero indicates a possible deviation from ΛCDM . Utilization of CPL for highly non-linear evolutions can, however, lead to erroneous conclusions. To demonstrate this the CPL parameterization was fit to a noiseless w evolution for the $\delta=3$, $w_0=-0.99$ case from this work. Figure 1 shows the results with the calculated w evolution as the solid line and the CPL fit as the dashed line. The CPL fit correctly indicates that ΛCDM is not a good fit to the evolution, but it does not contribute information about the actual evolution except that it is becoming more negative with time. More importantly the fit gives phantom values, w<-1, at scale factors greater than 0.8 for an evolution that has no phantom values.

Three recent MCMC analyses of observational data [13-15] with a CPL template find phantom values of w at low redshift. These results are interpreted by [14] as inconsistent with quintessence cosmologies since it is difficult for a quintessence cosmology to cross the phantom boundary [16]. This example highlights the need for accurate, analytic CPS templates rather than parameterizations of cosmological parameter evolution in dynamical cosmologies. In

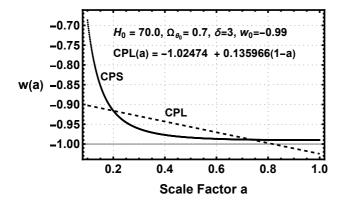


Figure 1. The dashed line is the CPL linear fit to the w(a) freezing evolution for $\delta = 3$ and $w_0 = -0.99$, solid line, from this work.

this case a possibly inaccurate conclusion is found based on a parameterization misfit rather than on physics based predictions. Analyses of the current and the expected new more precise and sensitive cosmological observations need accurate templates for proper interpretation of the data. This work concentrates on providing them.

4 The beta function formalism

The beta function formalism is based on commonalities between cosmological inflation and the particle physics based Renormalization Group, RG, flow [2–4]. In the formalism the beta function is a relationship between the dynamical scalar θ that is the source of dark energy and the scale factor a. In [2–4] beta is set to a common function such as a power law or an exponential and the resulting evolutions are explored. Here the potential is set and an appropriate beta function based on the potential is calculated to provide accurate evolutions for a specific cosmology and potential. The key is to use the beta function to determine $\kappa\theta(a)$ so that evolutions expressed in terms of the scalar are expressed in terms of the scale factor a. As described in the following this requires replacing the model potential with a potential, beta potential, that accurately but not exactly represents the model potential.

4.1 The beta function

The beta function in the flat quintessence cosmology formalism is defined as

$$\beta(\kappa\theta) \equiv \frac{d(\kappa\theta)}{d\ln(a)} = a\frac{d(\kappa\theta)}{da} \tag{4.1}$$

which defines a differential equation for $\theta(a)$ dependent on the form of $\beta(\theta)$. Even in this simple form it is apparent that

$$\frac{d(\kappa\theta)}{da} = \frac{\beta(\kappa\theta)}{a}, \qquad \frac{d(\kappa\theta)}{dt} = H\beta = \frac{1}{a}\frac{da}{dt}a\frac{d(\kappa\theta)}{da} = \kappa\dot{\theta}$$
 (4.2)

from the definition of the Hubble parameter H. The first Friedmann constraint, see section 2.1.1, and equation 4.2 give

$$3H^{2} = \rho_{\theta} = \frac{\dot{\theta}^{2}}{2} + V(\theta) = \frac{\beta^{2}H^{2}}{2} + V(\theta)$$
(4.3)

where ρ_{θ} is the dark energy density. In the presence of mass $3H^2$ is replaced by $3\Omega_{\theta}H^2$. The potential $V(\theta)$ is then

$$V(\theta) = 3H^2 - \frac{\beta^2 H^2}{2} = 3H^2 (1 - \frac{\beta^2}{6}) = \rho_{\theta} (1 - \frac{\beta^2}{6})$$
 (4.4)

From [3] the potential and beta function are related by

$$V(\theta) = \exp\{-\int \beta(\theta')d\theta'\}(1 - \frac{\beta^2}{6})$$
(4.5)

that requires that either beta be the negative of the logarithmic derivative of the dark energy density or that the potential is defined by the beta function in equation 4.5. In general and in this specific case the integral equation that defines beta as the negative of the logarithmic derivative of the dark energy density does not have an analytic solution. Equation 4.5,however provides the opportunity to meet the goal of accurate analytic evolutionary templates. Setting the beta function to the negative of the logarithmic derivative of the model potential provides solutions for a cosmology with a dark energy potential that is the model potential multiplied by $(1 - \beta^2/6)$. If $\beta^2/6$ is small relative to one accurate but not exact solutions that satisfy the criterion of significant improvement over parameterizations are achieved. The evolutions are then exact for the beta potential and cosmology and are accurate for the model potential at an accuracy of $(1 - \frac{\beta^2}{6})$. An accuracy threshold of 99% is set for this study. For all of the cases in the study the beta potential matches the model potential to an accuracy of 99.6% or better.

4.1.1 The HI potential beta function

The model potential for the beta function is equation 2.7. Taking the negative of the logarithmic derivative of the model potential produces the beta function

$$\beta(\kappa\theta) = \frac{d\kappa\theta}{d\ln(a)} = \frac{-4\kappa\theta}{(\kappa\theta)^2 - (\kappa\delta)^2}$$
(4.6)

giving a differential equation for $\theta(a)$. $\beta(\kappa\theta)$ is not a function of M leaving M free to satisfy the boundary conditions. Equation 4.6 shows that the beta function is positive since $\delta > \theta$, therefore, θ is increasing toward δ . The beta function links the evolution of the scalar to the evolution of the scale factor via the differential equation 4.6. Using $\dot{\theta} = \beta H$ and $\rho_{\theta} = 3\Omega_{\theta} H^2$ equations 2.5 and 4.6 show that

$$\beta(\kappa\theta) = \sqrt{3\Omega_{\theta}(w+1)} \tag{4.7}$$

Using the current values of the variables and parameters in equations 4.6 and 4.7 sets the current value of $\kappa\theta$.

$$\kappa \theta_0 = -\frac{4 - \sqrt{16 + 12\Omega_{\theta_0}(w_0 + 1)(\kappa \delta)^2}}{2\sqrt{3\Omega_{\theta_0}(w_0 + 1)}}$$
(4.8)

the positive solution of the equation since the square root term in the numerator is greater than four.

5 Parameter evolution derivations

The beta function 4.6 provides the means to derive the cosmological parameters as a function of the scale factor. Both Friedman constraints, section 2.1.1, are utilized in the derivations of the cosmological parameters. The first step is the derivation of $\kappa\theta(a)$. Section 5.1 shows that $\theta(a)$ is a function of the Lambert W function W(a). Parameters of $\theta(a)$ are also derived as functions of W(a) by substituting the proper function of W(a) for $\theta(a)$. The resulting functions of W(a) are reduced from the pure substitution to simplified expressions, if possible, without explicitly displaying the intermediate calculations to save space.

5.1 $\kappa\theta$ as a function of the scale factor

The analysis in this section utilizes the quintessence relationships described in section 2.1 and is therefore strictly valid only for flat quintessence. Rearranging equation 4.6 gives

$$4d(\ln(a)) = -\frac{(\kappa\theta)^2 - (\kappa\delta)^2}{\kappa\theta} d(\kappa\theta)$$
 (5.1)

Integrating both sides of eqn. 5.1 over 1 to a on the left and θ_0 to θ on the right gives

$$8\ln(a) = 2(\kappa\delta)^2 \ln(\kappa\theta) - (\kappa\theta)^2 - (2(\kappa\delta)^2 \ln(\kappa\theta_0) - \kappa\theta_0^2)$$
(5.2)

where $\kappa\theta_0$ is given in equation 4.8.

Setting the constant $2(\kappa\delta)^2 \ln(\kappa\theta_0) - \kappa\theta_0^2$ to c and dividing both sides by $(\kappa\delta)^2$ yields

$$\frac{8}{(\kappa\delta)^2}\ln(a) + \frac{c}{(\kappa\delta)^2} = 2\ln(\kappa\theta) - \frac{(\kappa\theta)^2}{(\kappa\delta)^2}$$
 (5.3)

Taking the exponential of both sides of eqn. 5.3 and dividing by $-(\kappa\delta)^2$ produces

$$-\frac{a^{\frac{8}{(\kappa\delta)^2}}}{(\kappa\delta)^2}e^{\frac{c}{(\kappa\delta)^2}} = -(\frac{\theta}{\delta})^2 e^{-(\frac{\theta}{\delta})^2}$$
(5.4)

Equation 5.4 has the form of the Lambert W function which is the solution to the equation

$$x = W(x)e^{W(x)} (5.5)$$

where here

$$x = -\frac{a^{\frac{8}{(\kappa\delta)^2}}}{(\kappa\delta)^2} e^{\frac{c}{(\kappa\delta)^2}} \qquad W(x) = -(\frac{\theta}{\delta})^2$$
 (5.6)

The Lambert W function commonly appears in cosmology and general relativity so its appearance here has a degree of naturalness.

The analytic solution for $\kappa\theta(a)$ is

$$\kappa\theta(a) = \kappa\delta\sqrt{-W(-\frac{a^{\frac{8}{(\kappa\delta)^2}}}{(\kappa\delta)^2}e^{\frac{c}{(\kappa\delta)^2}})}$$
(5.7)

that is the positive solution for the square root which is real since W(x) is negative.

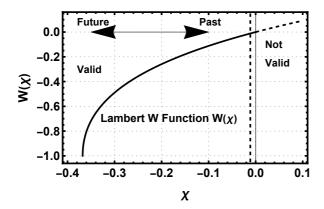


Figure 2. The Lambert W function showing the evolution for negative arguments which produce valid solutions for θ and positive arguments that produce invalid solutions, dashed line. The region between zero and the vertical dashed line at -0.0114 is the total range of χ for all of the cases in this study. The double arrow indicates the directions of future and past evolutions.

Negative values of W(x) occur if x is between $-\frac{1}{e}$ and zero [17], satisfied for all cases in this work. A concise form of equation 5.7 is

$$\kappa\theta(a) = \kappa\delta\sqrt{-W(qa^{\frac{8}{(\kappa\delta)^2}})}$$
 (5.8)

where a is the scale factor and the constant q is

$$q = -\frac{e^{\frac{c}{(\kappa\delta)^2}}}{(\kappa\delta)^2} \tag{5.9}$$

An even more concise notation is achieved by defining

$$\chi = qa^{\frac{8}{(\kappa\delta)^2}} \tag{5.10}$$

The scalar is then

$$\kappa\theta = \kappa\delta\sqrt{-W(\chi)}\tag{5.11}$$

Figure 2 shows the valid and invalid regions of the Lambert W function in eqn. 5.7. The value of χ is moving to the left with time in the figure after starting just negative of zero as indicated by the double arrow in the figure. The vertical dashed line shows the maximum excursion of χ for the cases in this study. Only a small portion of the valid χ values are occupied by the past leaving a large range for future evolution.

5.1.1 The beta function in terms of the Lambert W function

The beta function as a function of $\theta(a)$ is equation 4.6. Expressing it as a function of $W(\chi)$ demonstrates some of the common functional elements in terms of $W(\chi)$. The Lambert W function expression for $(\kappa\theta)^2$ is

$$(\kappa \theta)^2 = -(\kappa \delta)^2 W(\chi) \tag{5.12}$$

The often appearing $(\kappa\theta)^2 - (\kappa\delta)^2$ is then

$$(\kappa\theta)^2 - (\kappa\delta)^2 = -(\kappa\delta)^2 W(\chi) - (\kappa\delta)^2 = -(\kappa\delta)^2 (W(\chi) + 1)$$
(5.13)

resulting in a beta function of

$$\beta(W(\chi)) = \frac{4\sqrt{-W(\chi)}}{\kappa\delta(W(\chi) + 1)} \tag{5.14}$$

The scalar form of $(1 - \beta^2/6)$ is

$$1 - \frac{\beta^2(\theta)}{6} = 1 - \frac{8(\kappa\theta)^2}{3((\kappa\theta)^2 - (\kappa\delta)^2)^2}$$
 (5.15)

The Lambert W function form for $(1 - \beta^2/6)$ is

$$1 - \frac{8W(\chi)}{3\delta^2(W(\chi) + 1)^2} \tag{5.16}$$

5.1.2 Calculation of the potential constant M

At this point two potentials are defined, the model HI potential defined by equation 2.7 and the beta potential that is $(1 - \frac{\beta^2}{6})$ times the model potential. Their M parameters are termed M_{mod} and M_{β} respectively. In general the CPS templates are created using the beta potential. Further progress requires derivation of M_{β} . Since M_{β} is a constant the present day first Friedmann constraint determines M_{β} .

$$3\frac{H_0^2}{\kappa^2} = \rho_{\theta_0} + \rho_{m_0} \tag{5.17}$$

where the subscript 0 denotes the current value. Using eqn. 2.1 and 4.2, the present day constraint is

$$3H_0^2 = \frac{(H_0\beta(\kappa\theta_0))^2}{2} + M_\beta^4((\kappa\theta_0)^2 - \delta^2)^2(1 - \frac{\beta^2(\kappa\theta_0)}{6}) + \rho_{m_0}$$
 (5.18)

when rearranged is

$$3H_0^2(1 - \frac{\beta^2(\kappa\theta_0)}{6}) = M_\beta^4((\kappa\theta_0)^2 - \delta^2)^2(1 - \frac{\beta^2(\kappa\theta_0)}{6}) + \rho_{m_0}$$
 (5.19)

Solving for M_{β} gives

$$M_{\beta} = \sqrt{\frac{3\frac{H_0^2}{\kappa^2} - \frac{\rho_{m_0}}{(1 - \frac{\beta^2(\kappa\theta_0)}{6})}}{((\kappa\theta_0)^2 - (\kappa\delta)^2)^2}}$$
 (5.20)

The introduction of the matter density insures that the density in equation 4.4 is the dark energy density, not the total density. For completeness the model potential constant M_{mod} is

$$M_{mod} = \sqrt{\frac{\frac{3H_0^2}{\kappa^2} (1 - \frac{\beta^2(\kappa_0)}{6}) - \rho_{m_0}}{((\kappa\theta)^2 - (\kappa\delta)^2)^2}}$$
 (5.21)

5.2 The beta dark energy potential

Equation 5.22 shows the three individual polynomial terms of the beta potential $V_{\beta}(a)$.

$$V_{\beta}(\theta) = (M_{\beta}\kappa\theta)^4 - 2(M_{\beta}^2\kappa^2\theta\delta)^2 + (M_{\beta}\kappa\delta)^4(1 - \frac{\beta^2(\kappa\theta)}{6})$$
 (5.22)

In terms of the Lambert W function the beta potential is

$$V_{\beta}(a) = (M_{\beta}\kappa\delta)^{4}(W(\chi) + 1)^{2}(1 - \frac{8W(\chi)}{3(\kappa\delta)^{2}(W(\chi) + 1)^{2}}) = (M_{\beta}\kappa\delta)^{4}[(W(\chi) + 1)^{2} + \frac{8W(\chi)}{3(\kappa\delta)^{2}}]$$
(5.23)

5.3 The Hubble Parameter

Equations 2.6 provide the means to derive H(a) and H respectively. Similar to the calculation of M_{β} the first Friedmann constraint yields

$$3H(a)^{2}\left(1 - \frac{\beta^{2}(\kappa\theta)}{6}\right) = M_{\beta}^{4}((\kappa\theta)^{2} - \delta^{2})^{2}\left(1 - \frac{\beta^{2}(\kappa\theta)}{6}\right) + \frac{\rho_{m_{0}}}{a^{3}}$$
 (5.24)

The solution for H(a) is

$$H(a) = \sqrt{\frac{M_{\beta}^{4}((\kappa\theta)^{2} - (\kappa\delta)^{2})^{2} + \frac{\rho_{m_{0}}}{a^{3}(1 - \frac{\beta^{2}(\kappa\theta)}{6})}}{3}} = \frac{1}{\sqrt{3}}\sqrt{M_{\beta}^{4}((\kappa\theta)^{2} - (\kappa\delta)^{2})^{2} + \frac{\rho_{m_{0}}}{a^{3}(1 - \frac{8(\kappa\theta^{2})^{2}}{3((\kappa\theta)^{2} - (\kappa\theta)^{2})^{2}})}}$$
(5.25)

In terms of the Lambert W function

$$H(a) = \sqrt{\frac{(M_{\beta}\delta)^4 (W(\chi) + 1)^2 + \frac{\rho_{m_0}}{a^3 (1 + \frac{8W(\chi)}{3(\kappa\delta)^2 (W(\chi) + 1)^2})}}{3}}$$
 (5.26)

 H_0 is included in equation 5.26 via M_{β} as given in equation 5.20.

For H expanding the right hand side of eqn. 2.6 and using eqn. 2.3 gives

$$3\dot{H} + 3H^2 = -(\dot{\theta}^2 + \frac{\rho_{m_0}}{a^3} + 2p) \tag{5.27}$$

Since $3H^2$ is the sum of the dark energy and matter densities using eqn.2.1 for the dark energy pressure gives.

$$\dot{H}(a) = -\frac{1}{2}(\dot{\theta}^2 + \frac{\rho_{m_0}}{a^3}) = -\frac{1}{2}((\beta H)^2 + \frac{\rho_{m_0}}{a^3})$$
 (5.28)

5.4 The derivatives of θ

Although the time and scale factor derivatives of $\theta(a)$ are not observables they are required for the calculation of several observable parameters such as the dark energy density. The θ derivatives are derived from equations 4.2. Taking $\dot{\theta}$ as $\beta(\theta)H(\theta)$ yields

$$\dot{\theta}(a) = \frac{4\kappa\theta}{\sqrt{3}} \sqrt{M_{\beta}^4 + \frac{\rho_{m_0}}{a^3(((\kappa\theta)^2 - (\kappa\delta)^2)^2 - \frac{8(\kappa\theta)^2}{3})}}$$
(5.29)

and in terms of the Lambert W function

$$\dot{\theta}(a) = \frac{4\sqrt{-W(\chi)}}{\sqrt{3\kappa\delta}} \sqrt{(M_{\beta}\kappa\delta)^4 + \frac{\rho_{m_0}}{a^3((W(\chi)+1)^2 + \frac{8W(\chi)}{3(\kappa\delta)^2})}}$$
(5.30)

Also from equations 4.2 the derivative of $\theta(a)$ with respect to a is $\beta(a)/a$. In the $\theta(a)$ format

$$\frac{d(\kappa\theta(a)}{da} = \frac{-4\kappa\theta}{a(\kappa\theta)^2 - (\kappa\delta)^2}$$
 (5.31)

The Lambert W format is

$$\frac{d(\kappa\theta(a)}{da} = \frac{4\sqrt{-W(\chi)}}{\kappa\delta a(w(\chi)+1)}$$
(5.32)

Both the scalar $\theta(a)$ and its derivatives with respect to time and the scale factor are now available enabling derivation of cosmological parameters and fundamental constants as functions of either the scale factor a or the Lambert $W(\chi(a))$ function.

5.5 The dark energy density and pressure and the matter density

The dark energy and matter densities plus the pressure are important cosmological parameters. The matter density has the simple form

$$\rho_m(a) = \frac{\rho_{m_0}}{a^3} \tag{5.33}$$

where ρ_{m_0} is the current matter density. The dark energy density is given by eqns. 2.1 and 4.2.

$$\rho_{\theta} = \frac{\dot{\theta}^2}{2} + V = \frac{\beta^2 H^2}{2} + M_{\beta}^4 ((\kappa \theta)^2 - (\kappa \delta)^2)^2 (1 - \frac{\beta^2}{6})$$
 (5.34)

In terms of the scalar θ the dark energy density is

$$\frac{8(\kappa\theta)^{2}}{3}(M_{\beta}^{4} + \frac{\rho_{m_{0}}}{a^{3}(((\kappa\theta)^{2} - (\kappa\delta)^{2})^{2} - \frac{8(\kappa\theta)^{2}}{3})}) + M_{\beta}((\kappa\theta)^{2} - (\kappa\delta)^{2})^{2}(1 - \frac{8(\kappa\theta)^{2}}{3((\kappa\theta)^{2} - (\kappa\delta)^{2})^{2}})$$
(5.35)

and the Lambert W function form is

$$-\frac{8W(\chi)}{3(\kappa\delta)^2}[M_{\beta}\kappa\delta)^4 + \frac{\rho_{m_0}}{a^3((W(\chi)+1)^2 + \frac{8W(\chi)}{3(\kappa\delta)^2})}] + (M_{\beta}\kappa\delta)^4[(W(\chi)+1)^2 + \frac{8W(\chi)}{3(\kappa\delta)^2}]$$
(5.36)

The dark energy pressure is

$$P_{\theta} = \frac{\dot{\theta}^2}{2} - V = \frac{\beta^2 H^2}{2} - M_{\beta}^4 ((\kappa \theta)^2 - (\kappa \delta)^2)^2 (1 - \frac{\beta^2}{6}))$$
 (5.37)

The scalar form of the dark energy pressure is

$$P_{\theta} = \frac{8\theta^{2}}{3} \left[M_{\beta}^{4} + \frac{\rho_{m_{0}}}{a^{3} \left(((\kappa\theta)^{2} - (\kappa\delta)^{2})^{2} - \frac{8\theta^{2}}{3} \right)} \right] - M_{\beta}^{4} \left((\kappa\theta)^{2} - (\kappa\delta)^{2} \right)^{2} \left(1 - \frac{8\theta^{2}}{3((\kappa\theta)^{2} - (\kappa\delta)^{2})^{2}} \right)$$

$$(5.38)$$

The extra term in the dark energy pressure is because the $\frac{8(\kappa\theta)^2}{3(\kappa\delta)^2}M^4$ term that canceled in the dark energy density added in the dark energy pressure due to the change in sign of the potential. Using equation 5.23 and 5.30 the Lambert W forms of the pressure is

$$P_{\theta}(a) = -(M_{\beta}\kappa\delta)^{4} \left(\frac{16W(\chi)}{3(\kappa\delta)^{2}} + (W(\chi) + 1)^{2}\right) - \frac{8\rho_{m_{0}}W(\chi)}{a^{3}[3(\kappa\delta)^{2}(W(\chi) + 1)^{2} + 8W(\chi)]}$$
(5.39)

5.6 The Dark Energy Equation of State

The dark energy EoS is calculated directly from equation 2.2. Dividing through by the potential gives

$$w(a) = \frac{\frac{\theta(a)^2}{2V(a)} - 1}{\frac{\dot{\theta}(a)^2}{2V(a)} + 1}$$
 (5.40)

showing that when $\dot{\theta}(a)^2/2V(a)$ is small w(a) is near minus one. For most of the cases here $\dot{\theta}(a)^2/2V(a)$ does not get much larger than $(w_0 + 1)$. The exceptions are the $\delta = 3$ cases at small scale factors. In terms of the scalar $\theta \dot{\theta}(a)^2/2V(a)$ is

$$\frac{\dot{\theta}(a)^2}{2V(a)} = \frac{\frac{8(\kappa\theta)^2}{3} \left(M_{\beta}^4 + \frac{\rho_{m_0}}{a^3(((\kappa\theta)^2 - (\kappa\delta)^2)^2 - \frac{8(\kappa\theta)^2}{3})}\right)}{M_{\beta}^4((\kappa\theta)^2 - (\kappa\delta)^2)^2 \left(1 - \frac{8(\kappa\theta)^2}{3((\kappa\theta)^2 - (\kappa\delta)^2)^2}\right)}$$
(5.41)

Table 1. Boundary conditions and parameter values in this work. H_0 is the current value of the Hubble parameter in units of $\frac{km/sec}{Mpc}$. Ω_{m_0} and Ω_{ϕ_0} are the current ratios of the matter and dark energy densities to the critical density. w_0 are the current values of the dark energy equation of state and $\kappa\delta$ are the dimensionless constant values in the dark energy potential.

H_0	Ω_{m_0}	Ω_{θ_0}		w_0			$\kappa\delta$		scale factor a
70	0.3	0.7	-0.99	-0.995	-0.999	1	2	3	0.1 - 1.0

and

$$w(\kappa\theta) = \frac{\frac{8(\kappa\theta)^{2}}{3} \left(M_{\beta}^{4} + \frac{\rho_{m_{0}}}{a^{3}(((\kappa\theta)^{2} - (\kappa\delta)^{2})^{2} - \frac{8(\kappa\theta)^{2}}{3})}\right) - M_{\beta}^{4}((\kappa\theta)^{2} - (\kappa\delta)^{2})^{2} \left(1 - \frac{8(\kappa\theta)^{2}}{3((\kappa\theta)^{2} - (\kappa\delta)^{2})^{2}}\right)}{\frac{8(\kappa\theta)^{2}}{3} \left(M_{\beta}^{4} + \frac{\rho_{m_{0}}}{a^{3}(((\kappa\theta)^{2} - (\kappa\delta)^{2})^{2} - \frac{8(\kappa\theta)^{2}}{3})}\right) + M_{\beta}^{4}((\kappa\theta)^{2} - (\kappa\delta)^{2})^{2} \left(1 - \frac{8(\kappa\theta)^{2}}{3((\kappa\theta)^{2} - (\kappa\delta)^{2})^{2}}\right)}$$

$$(5.42)$$

Using equations 5.36 and 5.39 the Lambert W equation for $w(\chi)$ is

$$w(\chi) = \frac{-M_{\beta}^{4} \left(\frac{16W(\chi)}{3(\kappa\delta)^{2}} + (W(\chi) + 1)^{2}\right) - \frac{8\rho_{m_{0}}W(\chi)}{a^{3}(3(\kappa\delta)^{2}(W(\chi) + 1)^{2} + 8W(\chi))}}{M_{\beta}^{4}(W(\chi) + 1)^{2} - \frac{8\rho_{m_{0}}W(\chi)}{a^{3}(3(\kappa\delta)^{2}(W(\chi) + 1)^{2} + 8W(\chi))}}$$
(5.43)

5.7 The CPS templates

The functions for the cosmological parameters derived in this section form the set of CPS templates for flat quintessence and the HI potential. Appendix A gathers the templates together in an abbreviated form, giving the templates both as functions of $\theta(a)$ to display the physics and as functions of the Lambert W functions $W(\chi)$, where $\chi = qa^{\frac{8}{\delta^2}}$, to aid in template coding. The Lambert W function is a standard function in most mathematical coding platforms. The following section displays the evolutions of the observable and some of the unobservable cosmological parameters such as the scalar θ that are essential elements in the cosmology. Section 7 follows with the evolution of the fundamental constants α and μ .

6 Cosmological Parameter Evolution and Observations

The HI potential provides a rich set of evolutionary characteristics that are not obvious from their mathematical form in the templates. This section provides graphical presentations of the evolutions and comments on the observational consequences of the parameters for discriminating between static and dynamical dark energy. The evolutions are a strong function of the boundary conditions and the selection of relevant constants such as the HI potential constant δ .

6.1 Boundary conditions and constants

The boundary conditions and values of relevant constants are displayed in table 1. The boundary conditions are set at the current epoch and the constants are chosen to display the range of evolutions. The form of the evolutions is primarily controlled by two parameters, the current dark energy EoS, w_0 and the HI potential constant δ . The seemingly arbitrary choices for δ , 1, 2, and 3, display the three different characteristics of HI potential evolutions. Since discrimination between static and dynamical dark energy is a main subject of the study

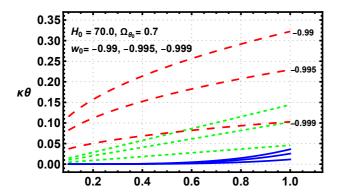


Figure 3. The evolution of the scalar $\kappa\theta(a)$ for all $\kappa\delta$ and w_0 values. The $\delta=1$ evolutions are solid tracks, blue, $\delta=2$ the dashed tracks, green and $\delta=3$ the long dashed tracks, red. These same line styles and colors are used to denote δ in the remaining figures unless stated otherwise. The w_0 values are indicated on the right for the $\delta=3$ tracks. For all δ values the $w_0=-0.99$ case has the greatest evolution and the $w_0=-0.999$ case has the least.

the w_0 values are placed close to minus one to show the difficulties of such discrimination. The choices for H_0 and Ω_{θ} are set to be close matches to concordance cosmology values. All are easily changed in the templates to suit other boundary conditions and constant choices.

6.2 The evolution of the scalar

The evolution of θ depends heavily on w_0 and δ . Figure 3 shows the evolution of the scalar for all combinations of w_0 and $\kappa\delta$ as a function of a. The $\delta=1$ evolution traces are solid lines, blue, $\delta=2$ dashed lines, green, and $\delta=3$ long dashed lines, red,. This format is retained in subsequent figures unless specified otherwise. The degree of evolution increases with larger values of δ and further deviation of w_0 from minus one. The second derivative of the slope changes from positive for $\delta=1$, to almost zero for $\delta=2$ to negative for $\delta=3$. This change in second derivative persists for most evolutions and results in non-monotonic evolution for the dark energy EoS not seen in previous monotonic potential calculations [18, 19]. The relative evolution of the scalar is quite small, particularly for the $\delta=1$ cases, consistent with a small value of $\dot{\theta}$. The values in fig. 3 are for $\kappa\theta$ which is not the true scalar. The true scalar is $M_{\beta}\kappa\theta$ where M_{β}^4 is the leading dimensional constant in the potential. Each combination of δ and w_0 requires a different value of M to meet all of the boundary conditions as shown by equation 5.20.

6.3 The evolution of the dark energy potential

Figure 4 shows the monotonically decreasing evolution of V(a) for all values of δ and w_0 . It also plots the evolution of the two dynamical terms $-2(M_{\beta}^2\kappa^2\theta\delta)^2$ and $(M_{\beta}\kappa\theta)^4$. The potential has very small changes over the range of scale factors. Though not required in the beta function formalism the potential conforms to the usual slow roll conditions. The polynomial form of the potential produces important differences from monomial potentials. The constant $(M_{\beta}\kappa\delta)^4$ is the dominant term since $\theta \ll \delta$ at the a values considered here. It is similar to a cosmological constant. The two dynamical terms are $-2(M_{\beta}^2\kappa^2\delta\theta)^2$ and $(M_{\beta}\kappa\theta)^4$ with the first term dominant over the second again due to $\delta > \theta$. For the $\delta = 1$ case the potential is essentially constant until the late time evolution considered in this work.

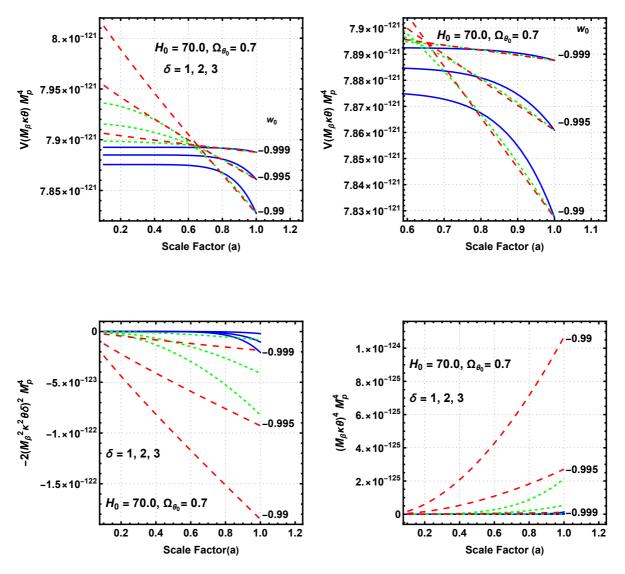


Figure 4. The top left panel shows the evolution of V(a) for all values of w_0 and δ . The values of w_0 are shown at the bottom right of the figures and the line styles are consistent with previous plots. The top right panel shows the late time evolution of the potential The bottom left plot shows the evolution of the first variable term $-2(\kappa^2 M_\beta^2 \theta \delta)^2$ and the bottom right plot is the second variable term $(M_\beta \kappa \theta)^4$. Note the changes in vertical scale in the bottom two plots.

6.4 The accuracy of the CPS templates

The CPS templates are exact and consistent solutions for the beta potential and the flat quintessence cosmology. The CPS templates are therefore accurate for the model potential to the degree that the beta potential is accurate for the model potential. The tradeoff of the beta potential for the model potential is deemed acceptable since it enabled the derivation of the scalar as an analytic function, the Lambert W function, in terms of the scale factor. No analytic beta function was found that produced the model potential in equation 4.5. The beta potential is simply $(1 - \beta^2/6)$ times the model potential therefore the accuracy is $(1 - \beta^2/6)$. Figure 5 shows the percentage accuracy that the beta potential represents the model potential for all cases.

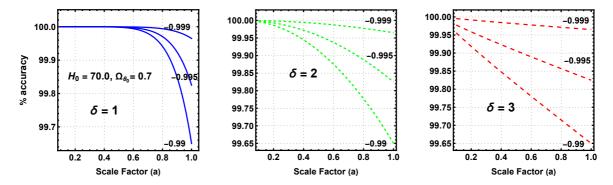


Figure 5. The figure shows the percentage accuracy that the beta potential represents the model potential for each value of δ .

The maximum deviation of the beta potential from the model potential is at the current epoch. The deviations for a given w_0 are all the same since the beta functions are all the same for a given w_0 . The a=1 percentage accuracies are 99.65, 99.825 and 99.965 for w_0 equal to -0.99, -0.995 and -0.999 with the accuracies for scale factor less than one all higher. The paths to the common a=1 accuracy differ for each δ . The accuracy of the $\delta=1$ case is essentially 100% up to a scale factor of 0.6 before evolving rapidly to the final accuracy at a=1. The $\delta=2$ cases deviate from 100% very early and evolve with increasing rapidity to the final value. The $\delta=3$ cases begin deviating from 100% at scale factors less than 0.1 and evolve linearly to the final values. The cosmological parameters set by the boundary conditions, however, are exactly correct at a=1.

6.5 The evolution of the Hubble parameter

Figure 6 shows the evolution of the Hubble parameter H(a) for all values of δ and w_0 plus Λ CDM. As found for other dark energy potentials [18, 19] the individual traces are indistinguishable at the resolution of the figure making the Hubble parameter a poor discriminator between static and dynamical dark energy. This indicates that the Hubble parameter is relatively insensitive to the dark energy potential, unlike most of the other parameters. This is partially due to fixing H at a=1 to H_0 and the dominance of matter over dark energy at redshifts greater than one. The deviations from Λ CDM are quantified in section 6.5.1 The dashed line in the figure shows the evolution of \dot{a} confirming that the transition from deceleration to acceleration of the expansion of the universe occurs at the observed epoch.

6.5.1 Deviations from Λ CDM

The percentage deviation of the dynamical dark energy Hubble parameter from Λ CDM, $\frac{H_{dyn}-H_{\Lambda}}{H_{\Lambda}}$, is a quantitative measure of the difference between the evolutions. Figure 7 shows the percentage deviations for all of the cases as a function of a. All deviations are less than 0.19% at their maximum and all of the $\delta=1$ deviations are less than 0.033%. The maximum deviation from Λ CDM for the $\delta=1$, $w_0=-0.999$ case is less than 0.0033%. This is not detectable with the current accuracy of H(a) measurements. Maximum deviations occur at smaller a as the value of δ increases. but all of the cases have maximum deviations at a greater than 0.5. For a given H_0 the deviation is zero at redshift zero by the boundary conditions and increases at higher redshifts. After a redshift of ≈ 1 matter density begins to dominate, decreasing the percentage deviation.

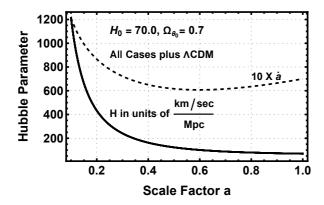


Figure 6. The evolution of H(a) for all values of w_0 and δ plus Λ CDM in units of (km/sec)/Mpc. The traces are indistinguishable at the resolution of the figure. The dashed track shows the evolution of $10 \times \dot{a}$ to indicate the transition from deceleration to acceleration of the expansion of the universe. The \dot{a} track is multiplied by 10 to make the transition visible at the scale of the plot.

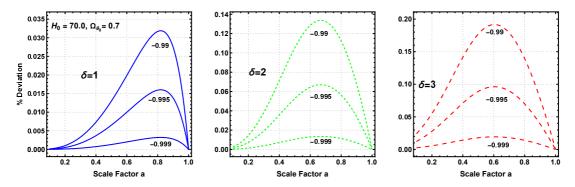


Figure 7. The evolution of the percentage difference between the HI Hubble parameter and Λ CDM for all values of w_0 and δ . Each of the three panels is for a specific δ .

6.5.2 Hubble parameter observational implications

For the w_0 values close to minus one in this study it is difficult to detect deviations from Λ CDM using only Hubble parameter observations. The peak deviations occur between scale factors of 0.6 and 0.8 dependent on the δ value and essentially independent of w_0 . This low redshift regions offers the best chance for observing departures from Λ CDM, particularly for higher deviations of w_0 from minus one than in this work at high δ values. Bringing w_0 closer to minus one reduces the deviations roughly as (w+1). This means that observational constraints on deviations of H from Λ CDM can be met by bringing w_0 closer to minus one while still maintaining a dynamical dark energy density. Falsifying dynamical dark energy with the Hubble parameter alone is very difficult. The $\delta = 1$, $w_0 = -0.999$ deviations are undetectable with current techniques. Peculiar motions at low redshift may be a complicating factor at the highest sensitive scale factors. The $\delta = 3$, $w_0 = -0.99$ deviations at 0.2% are most likely within reach with future observational techniques given that the current accuracy is on the order of 1km/sec [20].

6.6 Evolution of $\dot{\theta}$

Figure 8 shows the evolution of $M_{\beta}\kappa\dot{\theta}$ for the full range of a and for a between 0.4 and 1.0 to show the late time evolution in more detail. It is obvious that the a=1 $\dot{\theta}$ values for a specific

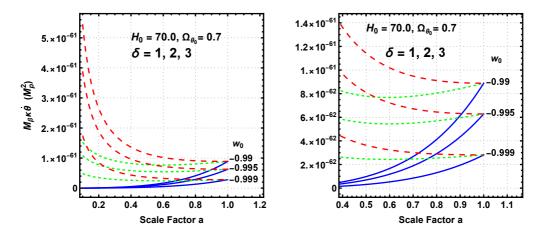


Figure 8. The evolution of the time derivative true scalar $M_{\beta}\kappa\dot{\theta}$ as a function of the scale factor for all values of δ and w_0 for the full scale factor range in the upper panel and in more detail for a between 0.4 and 1.0 in the lower panel.

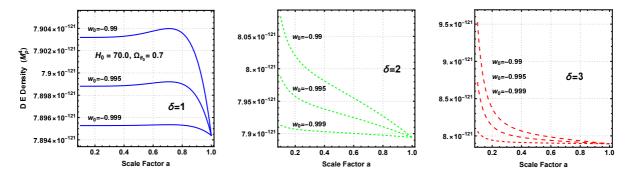


Figure 9. The evolution of the dark energy density ρ_{θ} as a function of the scale factor. The panels are for $\delta = 1, 2$, and 3 left to right.

 w_0 are equal because $H=H_0$ and the a=1 β values are the same for a given w_0 . The first derivative of the evolution changes from positive for $\delta=1$, transitioning from negative to positive for $\delta=2$ and negative for $\delta=3$. These changes are a primary driver for the changes in the second derivative in many of the cosmological parameters. This is particularly true for the dark energy EoS.

6.7 Evolution of the dark energy density

Figure 9 shows the evolution of the dark energy density for all of the cases. The evolutions are sensitive to the value of δ . The $\delta=1$ evolutions are quite flat for scale factors less than 0.5 with a slight non-monotonic rise before decreasing with a positive second derivative to the common point at a=1.0. The $\delta=2$ evolution is monotonically decreasing initially with a negative second derivative transitioning to a slightly positive second derivative near a=0.5. The $\delta=3$ evolution is monotonically decreasing with a negative second derivative at all plotted scale factors. The total change in the dark energy density is less than 0.1% for all of the $\delta=1$ cases, on the order of 1% for $\delta=2$ and on the order of 10% for $\delta=3$. As usual the closer w_0 is to minus one the less the evolution. The small percentage change of ρ_{θ} is consistent with the cases having evolutions similar to Λ CDM. The flat ρ_{θ} regions in the $\delta=1$ cases act like Λ CDM.

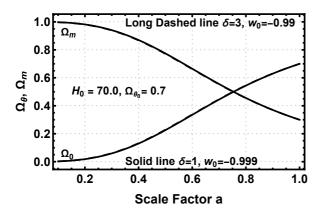


Figure 10. The evolution of Ω_{θ} and Ω_{m} for $\delta = 3$, $w_{0} = -0.99$, long dashed line and $\delta = 1$, $w_{0} = -0.999$ solid line. The tracks are indistinguishable at the resolution of the plot.

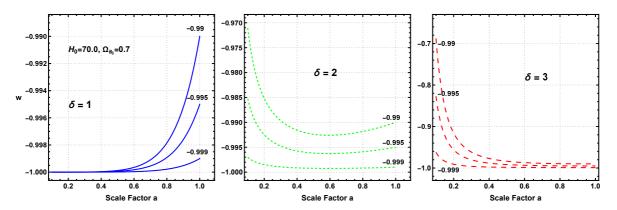


Figure 11. The evolution of w as a function of the scale factor a. The left to right panels are for $\delta = 1, 2,$ and 3. The w_0 values are indicated by numbers near the traces.

Figure 10 shows the evolution of Ω_m and Ω_{θ} for the two most extreme input values, $\delta = 3$, $w_0 = -0.99$, long dashed line and $\delta = 1$, $w_0 = -0.999$ solid line. The tracks are indistinguishable in the plot indicating they are relatively independent of δ and w_0 .

6.8 Evolution of the dark energy equation of state

The evolution of the dark energy EoS w is very dependent on the value of δ as shown in figure 11. The left panel of figure 11 shows the evolution for the $\delta=1$ cases. The $\delta=1$ cases are purely thawing at all scale factors in figure 11. Since they are thawing w_0 is its maximum deviation from minus one. For a<0.6 w is essentially minus one. These are the cases most similar to Λ CDM and the hardest to distinguish from a cosmological constant.

The $\delta=2$ cases in the middle panel transition from freezing to thawing at roughly a=0.5, giving a non-monotonic evolution of w. Their early time w values are higher than their w_0 values but their overall evolutions are almost as flat as the $\delta=1$ thawing cases. The right hand panel $\delta=3$ cases are classic freezing evolutions with w initially distant from minus one freezing toward minus one. Detection of their high deviations from minus one may be possible with the upcoming more precise observational measurements. Identification of the $\delta=3$ evolutions would be a strong case in favor of dynamical dark energy. The large

deviations from minus one, ≈ -0.7 at high redshift, offer the best chance of observational detection

The $\delta=1$ w evolutions illustrate the difficulty of falsifying dynamical dark energy through dark energy EoS observations. All of the $\delta=1$ cases have deviations from minus one that are too small to be detected by current observational techniques. Any non-zero constraint on deviations of w from minus one can be met by simply making w_0 closer to minus one but not exactly minus one On the other hand confirmation of a dynamical dark energy by observations establishing values of w not equal to minus one is strong evidence for a dynamical dark energy density. Another possibility is a detection of a temporal variation of fundamental constants such as the fine structure constant α or the proton to electron mass ratio μ discussed in section 7.

Figure 11 displays the versatility of the HI potential. The simple $\delta=1,\ 2,\ 3$ values were picked because they demonstrate the three types of evolution: pure thawing, transition from freezing to thawing and freezing. Intermediate values of δ provide smooth transitions between the three modes. This means that the HI potential CPS templates can easily cover the a large range of dark energy EoS evolutions.

7 Temporal evolution of fundamental constants

In the absence of special symmetries scalar fields that interact with gravity also interact with other sectors [21, 22]. The proton to electron mass ratio μ and the fine structure constant α values are determined by the Quantum Chromodynamic Scale Λ_{QCD} , the Higgs vacuum expectation value ν and the Yukawa couplings h [23]. Here it is assumed that the scalar responsible for dark energy also interacts with these sectors. The total of the interactions with the three particle physics parameters produces a coupling factor ζ_x , where x is either μ or α [23, 24]. Since the couplings are due to the same scalar field there is a relationship between the evolution of w and the evolution of μ and α described in section 7.1.

The relative change of the constants is given by eqn. 7.1.

$$\frac{\Delta x}{x} = \zeta_x (\kappa \theta - \kappa \theta_0) \tag{7.1}$$

This simple linear interaction can be thought of as the first term of a Taylor expansion of a more complex coupling. The only difference in the evolution of the constants is the strengths of ζ_{μ} and ζ_{α} The current limits on the variance of α and μ are $\Delta \alpha/\alpha = -(1.3 \pm 1.3_{stat} \pm 0.4_{sys}) \times 10^{-6}$, 1σ [25] at z = 1.15 and $\Delta \mu/\mu \leq \pm 1.1 \times 10^{-7}$ 2σ [26, 27] at z = 0.89. Both redshifts have look back times greater than half the age of the universe. The following analysis uses the more stringent limit on the variation of μ .

The left panel of figure 12 shows the evolution of $\Delta\mu/\mu$ as a function of the a for $\zeta_{\mu}=10^{-6}$. The error bar at a=0.53 is the 2σ observational $\Delta\mu/\mu$ constraint given above. All of the cases considered in this work satisfy the 2σ $\Delta\mu/\mu$ constraint, mainly due to the small deviation of w_0 from minus one. For larger deviations from minus one the $\delta=3$ cases start to violate the constraint. The $\delta=1$ cases are close to the constraint and improved measurements could produce constraints not satisfied by even the $\delta=1$ cases. These cases, however, can be brought back into compliance by reducing the particle physics coupling factor as covered in section 7.1. The coupling strength was chosen to be positive making the evolution negative but the opposite is equally likely. Consistent with equation 7.1 the second derivative of the evolution of μ is the same as the scalar θ .

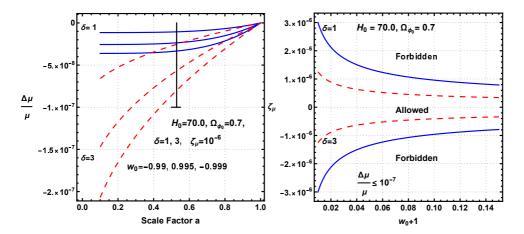


Figure 12. The left plot shows evolution of $\frac{\Delta\mu}{\mu}$ for the three w_0 values and δ values of 1 and 3. The $\delta=2$ evolution lies between the two but is not shown to avoid crowding. The error bar at a=0.53 extending from 0 to -1.1×10^{-7} is the 2σ observational constraint on $\frac{\Delta\mu}{\mu}$. The right plot shows the forbidden and allowed regions in the (w_0+1) , ζ_{μ} plane are shown for δ values of 1 (solid blue lines) and 3 (red long dashed lines, The regions between the positive and negative tracks for each δ value are allowed while the regions outside of the two tracks are forbidden.

7.1 Fundamental constant cosmological and new physics constraints

The evolution of the fundamental constants in a quintessence cosmology has a direct relationship to the evolution of the dark energy EoS. The evolution of $\Delta \mu/\mu$ is [28].

$$\frac{\Delta\mu}{\mu} = \zeta_{\mu} \int_{1}^{a} \sqrt{3\Omega_{\theta}(x)(w(x)+1)} x^{-1} dx \tag{7.2}$$

Equation 7.2 shows that μ or α varies whenever w is different than minus one even if the scalar is not varying with time. This makes α and μ w meters in the universe. The constraints on the temporal variation of the fundamental constants are constraints on the combination of the cosmological parameter w and the new physics coupling constant ζ_x . The fundamental constant constraints therefore define forbidden and allowed regions in a particle physics cosmological plane defined by ζ_x and w. The lack of a detected variance is consistent with but not a confirmation of Λ CDM. A detection of any variance of the fundamental constants, however, would signal the existence of new physics.

Making w_0 closer to minus one is a cosmological adjustment, lowering the value of ζ_{μ} is a new physics adjustment, setting w_0 to minus one and ζ_{μ} to zero is the standard model. The right panel of figure 12 shows the forbidden and allowed zones for $\delta=1$ and 3. It shows that there is significant space in the (w_0+1) - ζ_{μ} plane to satisfy the observational constraints with a dynamical cosmology The tracks between the allowed and forbidden zones are defined by

$$\zeta_{\mu} = \frac{\pm \frac{\Delta \mu}{\mu}}{\kappa \theta(a_{ob}, w_0, \Omega_{\theta_0}) - \kappa \theta_o(1, w_0, \Omega_{\theta_0})}$$
(7.3)

where a_{ob} is the a of the observation. The terms w_0 and Ω_{θ_0} appear due to their presence in eqn. 4.8 for θ_0 . The $\delta=2$ track lies between tracks for $\delta=1$ and 3. The higher δ values have greater $\Delta\theta$ and therefore tighter constraints. At the smallest plotted value of (w+1)=0.01 the ζ_{μ} magnitude for $\delta=3$ is constrained to $|\zeta_{\mu}|<\pm 1.22\times 10^{-6}$. The constraint on $\Delta\mu/\mu$ puts constraints on the temporal variation of the particle physics

parameters of $\Delta\Lambda_{QCD}/\Lambda_{QCD} \leq \pm 7.9 \times 10^{-5}$, $\Delta\nu/\nu \leq 7.9 \times 10^{-5}$ and $\Delta h/h \leq 4.9 \times 10^{-7}$ [24].

8 Conclusions

The beta function formalism provides a methodology for producing accurate evolutionary templates for a model dark energy potential using a beta function potential that is an accurate but not exact duplicate of the model potential. This methodology produced Cosmology and Potential Specific, CPS, templates for a flat quintessence cosmology with a model dark energy potential having the same mathematical form as the Higgs potential, the HI potential. CPS templates for the Hubble Parameter, the dark energy and matter densities, and the dark energy EoS were calculated for nine different combinations of the current dark energy EoS, w_0 and the HI potential constant δ as analytic functions of the scale factor a. These templates offer significantly improved accuracies relative to the parameterizations commonly used in likelihood calculation for dynamical cosmologies. They avoid the possibility of large errors in cosmology likelihoods by replacing parameterizations with specific cosmology and dark energy potential physics based templates. The new physics based CPS templates are good candidates for fiducial templates to discriminate between static and dynamical dark energy using the current and expected future cosmological parameter databases. With this purpose in mind the templates calculated in this work have current dark energy EoS values close to minus one to produce dynamical evolutions similar to the ΛCDM evolutions. Given the analytic functions presented in the text and assembled in appendix A CPS templates for a different set of boundary conditions are easily created. The methodology is also adaptable to the particular physics of other cosmologies and dark energy potentials.

The polynomial HI potential produces a wide range of cosmological parameter evolutions. A common feature of the evolutions are transitions of the sign of the second derivative of the evolution between negative and positive as a function of the constant δ in the HI potential. For the dark energy EoS w the second derivative is positive for $\delta = 1$, thawing, transitioning from negative to positive for $\delta = 2$, freezing to thawing, and negative for $\delta = 3$, freezing, producing a comprehensive range of w evolutions. At early times the constant term in the potential dominates, acting like a cosmological constant.

The evolution of the Hubble parameter is very similar to the Λ CDM evolution partly due to the choice of w_0 values close to minus one and partly that the Hubble parameter is relatively insensitive to the dark energy potential in a quintessence cosmology [18, 19]. This highlights the difficulty of using only the Hubble parameter to discriminate between static and dynamical dark energy density. The thawing w evolutions for the $\delta=1$ cases are similarly difficult to discriminate from Λ CDM since w is initially at minus one and only evolves away from minus one at late times to meet their w_0 almost minus one boundary conditions. Appendix A contains an abridged version of a CPS template suite for flat quintessence with the HI dark energy potential.

The $\delta=1$ CPS templates, particularly with $w_0=-0.999$ are excellent checks on whether dynamical cosmologies can achieve the same likelihoods as Λ CDM. This property makes these CPS templates good candidates for standard tests in all likelihood calculations that involve discrimination between static and dynamical dark energy. Lower likelihoods for these templates relative to Λ CDM can be due to a lower likelihood of quintessence and the HI potential as opposed to evidence for static dark energy.

The cosmological and particle physics constraints from the observed limits on the temporal evolution of the fundamental constant α and μ are also calculated. All cases studied here met these limits for the most stringent limit on $\Delta\mu/\mu$ with a coupling constant of 10^{-6} . All of the $\delta=3$ cases, however, would have failed if the coupling constant was a factor of two higher. The constraint on $\Delta\mu/\mu$ imposes both a cosmological constraint on w and a particle physics constraint on temporal evolution on the Quantum Chromodynamic Scale Λ_{QCD} , the Higgs vacuum expectation value ν and the Yukawa couplings h that comprise the coupling constant ζ_{μ} . These define an allowed area in the ζ_{μ} - (w_0+1) plane that constrains both cosmology and particle physics. The allowed regions shown in Figure 12 include Λ CDM and the standard model at the 0.,0. origin but also retain significant space for a dynamical dark energy as well.

Acknowledgments

The author would like to acknowledge the very useful and informative discussion with Sergey Cherkis on the mathematical properties of the Lambert W function.

References

- [1] National Academies of Sciences, Engineering, and Medicine 2021. Pathways to Discovery in Astronomy and Astrophysics for the 2020s. Washington, DC: The National Academies Press. https://doi.org/10.17226/26141.(2021)
- [2] Binetruy, P., Kirtsis, E., Mabillard, J., Pieroni, M. & Rosset, C., Universiality classes for models of Infation, JCAP1504 (2015) no. 04, 033-64
- [3] Cicciarella, F. & Pieroni, M., Universality for quintessence, JCAP1708 (2017) no. 8, 010-039
- [4] Kohri, K. and Matsui, H. Cosmological constant problem and renormalized vacuum energy density in curved background, JCAP, 06, (2017), 006, [arXiv:1612.08818]
- [5] Binetruy, P., Mabillard, J., & Pieroni, M., Universiality in generalized models of inflation, JCAP03060 (2017)
- [6] Copeland, E. J., Sami, M. and Tsujikawa, S., Dynamics of dark energy, Int. J. Mod. Phys. D 15 (2006) 1753 [hep-th/0603057v3].
- [7] Bahamonde, S., Bohmery, C. G., Carloniz, S., Copeland, E. J., Fang, W. and Tamaninik, N., Dynamical systems applied to cosmology: Dark energy and modified gravity Physics Reports, 775-777 (2018) 1 [arXiv:1712.03107]
- [8] Ratra, B. and Peebles, P.J.E., Cosmological consequences of a rolling homogeneous scalar field, Phys. Rev. D,37 (1988), 12, 3406
- [9] Peebles, P. J. E., and Ratra, B. Cosmology with a Time-Variable Cosmological Constant, Ap.J 325 (1988) L17
- [10] Chevallier, M. and Polarski, C., Accelerating universes with scaling dark matter, Int. J. Mod. Phys. D 10 (2001) 213 [gr-qc/0009008v2].
- [11] Linder, E.V., Exploring the expansion history of the universe, Phys. Rev. Let. **90** (2003) 091301.
- [12] Martinelli, M., Martins, C.J.A.P., Nesseris, S. and 92 additional authors, Euclid: constraining dark energy coupled to electromagnetism using astrophysical and laboratory data? ,[arxiv:2105.09746].

- [13] Planck Collaboration, Planck 2018 results, VI. Cosmological Parameters, A&A. 641 (2020) A6 [astro-ph.CO/:1807.06209v4].
- [14] Di Valentino, E., Melchiorri, A. and Silk, J., Cosmolgical constraints in extended parameter space from the Planck 2018 Legacy release JCAP 01, (2020) 13, 1 arXiv:1908.01391v2 [astro-ph.CO]
- [15] Di Valentino, E. A combined analysis of the Ho late time direct measurements and the impact on the Dark Energy sector MNRAS 502, (2020), 2065, arXiv:2011.00246v4 [astroph.CO].
- [16] Vikman, A. Can dark energy evolve to the phantom? Phys. Rev. D 71 (2005) 023515, [arXiv:astro-ph/0407107]
- [17] Olver, F. W. F., Lozier, D. W., Boisvert, R.F., and Clark, C.W., 2010, in *NIST Handbook of Mathematical Functions*, Chap. 4, p. 111, 1st ed, (Cambridge University Press, New York)
- [18] Thompson, R.I., Beta function quintessence cosmological parameters and fundamental constants I Power and inverse power law dark energy potentials, MNRAS 477, (2018), 4104, [astro-ph.CO/ 1804.02412v1]
- [19] Thompson, R.I., Beta function quintessence cosmological parameters and fundamental constants II. Exponential and logarithmic dark energy potentials, MNRAS 482, (2019), 5448, [astro-ph.CO/ 1811.03164v1]
- [20] Riess, Adam G.; Yuan, Wenlong; Macri, Lucas M.; Scolnic, Dan; Brout, Dillon; Casertano, Stefano; Jones, David O.; Murakami, Yukei; Breuval, Louise; Brink, Thomas G.; Filippenko, Alexei V.; Hoffmann, Samantha; Jha, Saurabh W.; Kenworthy, W. D'arcy; Mackenty, John; Stahl, Benjamin E.; Zheng, Weikang A Comprehensive Measurement of the Local Value of the Hubble Constant with 1 km/s/Mpc Uncertainty from the Hubble Space Telescope and the SH0ES Team arXiv:2112.04510
- [21] Carroll, S. M., Quintessence and the rest of the world: Suppressing long-range interactions, Phys. Rev., Lett., 81 (1998), 3067, [arXiv:astro-ph/9806099]
- [22] Figueroa, D., Florio, A., Opferkuch, T. and Stefanek, B. A. *Inconsistency of an inflationary sector coupled only to Einstein gravity*, *JCAP* **10** 92019) 011f arXiv:1811.04093
- [23] Coc, A., Nunes, N., Olive, K.A., Uzan, J-P, and Vangioni, E., Coupled variations of fundamental constants and primordial nucleosynthesis, Phys. Rev. D 76 (2007) 023511, [astro-ph/0610733]
- [24] Thompson, R.I., Fundamental constant observational bounds on the variability of the QCD scale, MNRAS 467, (2017), 4558, [astro-ph.CO/1702.06132v1]
- [25] Murphy, M. et. al. Fundamental physics with ESPRESSO: Precise limit on variations in the fine-structure constant towards the bright quasar HE 0515-4414, (2021), arXiv:2112.05819v1
- [26] Bagdonaite, J., Dapra', M., Jansen, P., Bethlem, H. L., Ubachs, W., Muller, S., Henkel, C. and Menten, K. M. Robust Constraint on a Drifting Proton-to-Electron Mass Ratio at z = 0:89 from Methanol Observation at Three Radio Telescopes Phys. Rev. Let. 111, (2013) 231101, arXiv:1311.3438
- [27] Kanekar, N., Ubachs, W., Menten, K. M., Bagdonaite, J., Brunthaler, A., Henkel, C., Muller, S., Bethlem, H.L., and Dapra, M. Constraints on changes in the proton-electron mass ratio using methanol lines MNRAS, 448, (2015), L104, arXiv:1412.7757
- [28] Thompson, R.I., Constraining cosmologies with fundamental constants I. Quintessence and K-essence, MNRAS 428, (2013), 2232, arXiv:1210.3031

CPS templates in $W(\chi)$

 $W(\chi)$, the solution to $\chi = W(\chi)e^{W(\chi)}$, is a central function for quintessence with the HI potential. The variable $\chi = -\frac{a^{\frac{8}{(\kappa\delta)^2}}}{(\kappa\delta)^2}e^{\frac{c}{(\kappa\delta)^2}}$. It can be written with three parameters: the scale

factor a, the constant δ and a compound constant $q = -\frac{e^{\frac{c}{(\kappa\delta)^2}}}{(\kappa\delta)^2}$ where c is defined in the main text and given below.. The boundary conditions are in table 1. The dimensionless scalar is $\kappa\theta$ and the subscript 0 indicates the value at the present time. In the following the first function is the parameter or constant in terms of θ and the second is in terms of $W(\chi)$.

The scalar field $\kappa\theta$

$$\kappa\theta, \qquad \kappa\delta\sqrt{-W(\chi)}.$$

The current $\kappa\theta$, $\kappa\theta_0$

$$-\frac{4-\sqrt{16+12\Omega_{\theta_0}(w_0+1)(\kappa\delta)^2}}{2\sqrt{3\Omega_{\theta_0}(w_0+1)}}$$
 Not a function of $W(\chi)$

The c parameter

$$2(\kappa\delta)^2 \ln(\kappa\theta_0) - \kappa\theta_0^2$$

Not a function of $W(\chi)$

The q parameter

$$q = -\frac{e^{\frac{c}{(\kappa\delta)^2}}}{(\kappa\delta)^2}$$

 $d(\kappa\theta)/da$

$$\frac{-4\kappa\theta}{a((\kappa\theta)^2 - (\kappa\delta)^2)}, \qquad \frac{4\sqrt{-W(\chi)}}{a\kappa\delta(W(\chi) + 1)}$$

The beta function

The beta function
$$\frac{-4\kappa\theta}{(\kappa\theta)^2 - (\kappa\delta)^2}, \qquad \frac{4\sqrt{-W(\chi)}}{\kappa\delta(W(\chi)+1)}$$

$$1 - rac{eta^{\mathbf{2}}(\mathbf{a})}{6}$$

$$1 - \frac{\beta(\kappa\theta)^{2}}{6}$$

$$1 - \frac{8(\kappa\theta)^{2}}{3((\kappa\theta)^{2} - (\kappa\delta)^{2})^{2}}, \qquad 1 + \frac{8W(\chi)}{3\delta^{2}(W(\chi) + 1)^{2}}$$

The model HI potential

$$M_m^4((\kappa\theta)^2 - (\kappa\delta)^2)^2, \qquad (M_m\kappa\delta)^4(W(\chi) + 1)^2$$

The model potential coefficient \mathcal{M}_m

$$\sqrt[4]{\frac{3H_0^2(1-\frac{\beta^2(\kappa\theta_0)}{6})-\rho_{m_0}}{((\kappa\theta_0)^2-(\kappa\delta)^2)^2}},$$
 Not a function of $W(\chi)$

The beta potential

$$M_{\beta}^{4}((\kappa\theta)^{2}-(\kappa\delta)^{2})^{2}(1-\frac{8(\kappa\theta^{2})^{2}}{3((\kappa\theta)^{2}-(\kappa\theta)^{2})^{2}}),$$
 $(M_{\beta}\kappa\delta)^{4}((W(\chi)+1)^{2}+\frac{8W(\chi)}{3(\kappa\delta)^{2}})$

The beta potential coefficient M_{β}

$$\sqrt[4]{\frac{3\frac{H_0^2}{\kappa^2} - \frac{\rho m_0}{(1 - \frac{8(\kappa\theta^2)}{3((\kappa\theta)^2 - (\kappa\theta)^2)^2})}}{((\kappa\theta_0)^2 - (\kappa\delta)^2)^2}}$$
Not a function of $W(\chi)$

The Hubble Parameter

$$\frac{1}{\sqrt{3}}\sqrt{M_{\beta}^{4}((\kappa\theta)^{2}-(\kappa\delta)^{2})^{2}+\frac{\rho_{m_{0}}}{a^{3}(1-\frac{8(\kappa\theta^{2}}{3((\kappa\theta)^{2}-(\kappa\theta)^{2})^{2}})}}, \quad \frac{1}{\sqrt{3}}\sqrt{(M_{\beta}\delta)^{4}(W(\chi)+1)^{2}+\frac{\rho_{m_{0}}}{a^{3}(1+\frac{8W(\chi)}{3\delta^{2}(W(\chi)+1)^{2}})}}$$

The time derivative of θ , $\dot{\theta}$

$$\frac{4\kappa\theta}{\sqrt{3}}\sqrt{M_{\beta}^{4} + \frac{\rho_{m_{0}}}{a^{3}(((\kappa\theta)^{2} - (\kappa\delta)^{2})^{2} - \frac{8(\kappa\theta)^{2}}{3})}}, \qquad \dot{\theta}(a) = \frac{4\sqrt{-W(\chi)}}{\sqrt{3}\kappa\delta}\sqrt{(M_{\beta}\kappa\delta)^{4} + \frac{\rho_{m_{0}}}{a^{3}((W(\chi)+1)^{2} + \frac{8W(\chi)}{3(\kappa\delta)^{2}})}}$$

The dark energy density

$$\frac{8(\kappa\theta)^{2}}{3} \left(M_{\beta}^{4} + \frac{\rho_{m_{0}}}{a^{3}(((\kappa\theta)^{2} - (\kappa\delta)^{2})^{2} - \frac{8(\kappa\theta)^{2}}{3})} \right) + M_{\beta}((\kappa\theta)^{2} - (\kappa\delta)^{2})^{2} \left(1 - \frac{8(\kappa\theta)^{2}}{3((\kappa\theta)^{2} - (\kappa\delta)^{2})^{2}} \right) ,$$

$$- \frac{8W(\chi)}{3(\kappa\delta)^{2}} \left[M_{\beta}\kappa\delta \right)^{4} + \frac{\rho_{m_{0}}}{a^{3}((W(\chi)+1)^{2} + \frac{8W(\chi)}{3(\kappa\delta)^{2}})} \right] + \left(M_{\beta}\kappa\delta \right)^{4} \left[(W(\chi)+1)^{2} + \frac{8W(\chi)}{3(\kappa\delta)^{2}} \right]$$

The dark energy pressure

$$\frac{8(\kappa\theta)^{2}}{3}(M_{\beta}^{4} + \frac{\rho_{m_{0}}}{a^{3}(((\kappa\theta)^{2} - (\kappa\delta)^{2})^{2} - \frac{8(\kappa\theta)^{2}}{3})}) - M_{\beta}((\kappa\theta)^{2} - (\kappa\delta)^{2})^{2}(1 - \frac{8(\kappa\theta)^{2}}{3((\kappa\theta)^{2} - (\kappa\delta)^{2})^{2}}),$$

$$-(M_{\beta}\kappa\delta)^{4}(\frac{16W(\chi)}{3(\kappa\delta)^{2}} + (W(\chi) + 1)^{2}) - \frac{8\rho_{m_{0}}W(\chi)}{a^{3}[3(\kappa\delta)^{2}(W(\chi) + 1)^{2} + 8W(\chi)]}$$

The matter density

$$\frac{\rho_{m_0}}{a^3}$$
, Not a function of $W(\chi)$

The dark energy equation of state

$$\begin{split} &\frac{8(\kappa\theta)^2}{3} (M_{\beta}^4 + \frac{\rho_{m_0}}{a^3(((\kappa\theta)^2 - (\kappa\delta)^2)^2 - \frac{8(\kappa\theta)^2}{3})}) - M_{\beta}((\kappa\theta)^2 - (\kappa\delta)^2)^2 (1 - \frac{8(\kappa\theta)^2}{3((\kappa\theta)^2 - (\kappa\delta)^2)^2}) \\ &\frac{8(\kappa\theta)^2}{3} (M_{\beta}^4 + \frac{\rho_{m_0}}{a^3(((\kappa\theta)^2 - (\kappa\delta)^2)^2 - \frac{8(\kappa\theta)^2}{3})}) + M_{\beta}((\kappa\theta)^2 - (\kappa\delta)^2)^2 (1 - \frac{8(\kappa\theta)^2}{3((\kappa\theta)^2 - (\kappa\delta)^2)^2}) \\ &- (M_{\beta}\kappa\delta)^4 (\frac{16W(\chi)}{3(\kappa\delta)^2} + (W(\chi) + 1)^2) - \frac{8\rho_{m_0}W(\chi)}{a^3[3(\kappa\delta)^2(W(\chi) + 1)^2 + 8W(\chi)]} \\ &- \frac{8W(\chi)}{3(\kappa\delta)^2} [M_{\beta}\kappa\delta)^4 + \frac{\rho_{m_0}}{a^3((W(\chi) + 1)^2 + \frac{8W(\chi)}{3(\kappa\delta)^2})}] + (M_{\beta}\kappa\delta)^4 [(W(\chi) + 1)^2 + \frac{8W(\chi)}{3(\kappa\delta)^2}] \end{split}$$